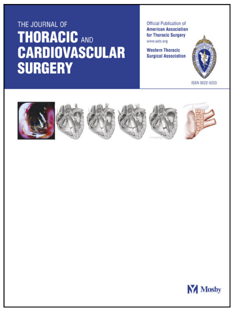

How Successful is Successful? Aortic Arch Shape Following Successful Aortic Coarctation Repair Correlates with Left Ventricular Function

Jan L. Bruse, MSc, Abbas Khushnood, MD, Kristin McLeod, PhD, Giovanni Biglino, PhD, Maxime Sermesant, PhD, Xavier Pennec, PhD, Andrew M. Taylor, MD, Tain-Yen Hsia, MD, Silvia Schievano, PhD, for the Modeling of Congenital Hearts Alliance (MOCHA) Collaborative Group

PII: S0022-5223(16)31136-9
DOI: 10.1016/j.jtcvs.2016.09.018
Reference: YMTC 10886

To appear in: *The Journal of Thoracic and Cardiovascular Surgery*

Received Date: 26 May 2016
Revised Date: 14 July 2016
Accepted Date: 7 September 2016

Please cite this article as: Bruse JL, Khushnood A, McLeod K, Biglino G, Sermesant M, Pennec X, Taylor AM, Hsia T-Y, Schievano S, for the Modeling of Congenital Hearts Alliance (MOCHA) Collaborative Group, How Successful is Successful? Aortic Arch Shape Following Successful Aortic Coarctation Repair Correlates with Left Ventricular Function, *The Journal of Thoracic and Cardiovascular Surgery* (2016), doi: 10.1016/j.jtcvs.2016.09.018.

Original Manuscript

Title: **How Successful is Successful? Aortic Arch Shape Following Successful Aortic Coarctation Repair Correlates with Left Ventricular Function**

Authors (max. 7): Jan L Bruse, MSc[1], Abbas Khushnood, MD[1], Kristin McLeod, PhD[2,3], Giovanni Biglino, PhD[1], Maxime Sermesant, PhD[3], Xavier Pennec, PhD[3], Andrew M Taylor, MD[1], Tain-Yen Hsia, MD[1*], and Silvia Schievano, PhD[1]; for the Modeling of Congenital Hearts Alliance (MOCHA) Collaborative Group[4]

Institutions and Affiliations: [1]Centre for Cardiovascular Imaging, University College London, Institute of Cardiovascular Science & Cardiorespiratory Unit, Great Ormond Street Hospital for Children, London, UK

[2]Simula Research Laboratory, Cardiac Modeling Department, Oslo, Norway

[3]Inria, Asclepios Team, Sophia Antipolis, France

[4]MOCHA Collaborative Group: Andrew Taylor, Sachin Khambadkone, Silvia Schievano, Marc de Leval, T. -Y. Hsia (University College London, UK); Edward Bove, Adam Dorfman (University of Michigan, USA); G. Hamilton Baker, Anthony Hlavacek (Medical University of South Carolina, USA); Francesco Migliavacca, Giancarlo Pennati, Gabriele Dubini (Politecnico di Milano, Italy); Alison Marsden (University of California, USA); Irene Vignon-Clementel (INRIA, France); Richard Figliola (Clemson University, USA).

Meeting Presentation: AATS 96th Annual Meeting, May 14-18, 2016, Baltimore, MD

Word Count (body):3335

Funding and Conflicts of Interest:
This work received funding support from Leducq Foundation (France), FP7 integrated project MD-Paedigree (European Commission) and National Institute of Health Research (UK). All authors have nothing to disclose regarding possible conflicts of interest.

*Corresponding author:
T-Y Hsia, MD
Cardiac Unit
Great Ormond Street Hospital for Children, NHS Trust
London, WC1N 3JH, UK
Telephone: +44-(0)207-813-8159
Email: hsiat@gosh.nhs.uk

Abstract

Objectives: Even after successful aortic coarctaion (CoA) repair, there remains a significant incidence of late systemic hypertension and other morbidities. Independent of residual obstruction, aortic arch morphology alone may impact on cardiac function and outcome. We sought to uncover the relationship of arch three-dimensional (3D) shape features with functional data obtained from cardiac magnetic resonance (CMR) scans.

Methods: 3D aortic arch shape models of 53 patients (mean age 22.3±5.6 years) 12-38 years following CoA repair were reconstructed from CMR data. A novel validated statistical shape analysis method computed a 3D mean anatomic shape of all aortic arches, and calculated deformation vectors of the mean shape towards each patient's arch anatomy. From these deformations, 3D shape features most related to left ventricular ejection fraction (LVEF), indexed left ventricular end diastolic volume (iLVEDV), indexed left ventricular mass (iLVM), and resting systolic blood pressure (BP) were extracted from the deformation vectors via partial least squares regression.

Results: Distinct arch shape features correlated significantly with LVEF ($r=0.42$, $p=0.024$), iLVEDV ($r=0.65$, $p<0.001$) and iLVM ($r=0.44$, $p=0.014$). Lower LVEF, larger iLVEDV and increased iLVM were identified with an aortic arch shape that has an elongated ascending aorta with high arch height-to-width ratio, a relatively short proximal transverse arch, and a relatively dilated descending aorta. High BP appeared to be linked to gothic arch shape features, but this did not achieve statistical significance.

Conclusions: Independent of hemodynamically important arch obstruction or residual CoA, specific aortic arch shape features late after successful CoA repair appears to be associated with worse left ventricular function. Analyzing 3D shape information via statistical shape modeling can be an adjunct to long-term risk assessment in patients following CoA repair.

Abbreviations and Acronyms

2D	2-dimensional
3D	3-dimensional
CMR	Cardiovascular Magnetic Resonance
CoA	Coarctation of the Aorta
LVEF	Left ventricular ejection fraction
iLVEDV	Indexed left ventricular end diastolic volume
iLVM	Indexed left ventricular mass
BP	Resting systolic blood pressure
SSM	Statistical Shape Model(ling)
E-E	End-to-end anastomosis
ExtE-E	Extended end-to-end anastomosis

Introduction

Despite being perceived as a straightforward lesion with proven and reproducible corrective surgical and interventional techniques, coarctation of the aorta (CoA) remains a clinical challenge due to a well-recognized high incidence of late complications and morbidities, even after successful repair. (1-4) In late follow-up, multiple studies have now demonstrated a persistence of chronic difficult-to-treat systemic hypertension with associated left ventricular hypertrophy, reduced exercise capacity, and progressive diastolic heart failure. (3-6) Therefore, long after a 'successful' isolated CoA repair with no residual anatomical or hemodynamic obstruction, a significant portion of these patients do not have a 'successful' cardiovascular life, requiring a life-long monitoring and chronic pharmacological management.

As part of the efforts to delineate contributing factors to the CoA puzzle, several investigators have examined the role of aortic arch shape. Discounting the obvious negative effects of residual stenosis or hypoplasia, certain morphologies, or appearance, of the surgically reconstructed aortic arch following isolated CoA repair has been identified to be associated with worse clinical outcome. (7-13) For example, the much ascribed "gothic" aortic arch with its exaggerated height-to-width ratio and distinct angulation at the crest is very likely less desirable than a more rounded and smoother 'romanesque' arch. Despite appearing logical and obvious, conclusive association between systemic hypertension and gothic arch shape remained elusive, with additional confounding issues of transverse arch and isthmus sizes adding to the controversy. (10, 14) It is most likely that a large part of these discrepant observations is due to the fact that majority of these studies applied traditional shape analysis based on linear two-dimensional (2D) measurements. Being widely variable in shape, angles, and size in three dimensions (3D), surgically reconstructed aortic arches following CoA repair cannot be adequately analyzed by traditional morphometric methods using a ruler to measure lengths and diameters, since these are insufficient to provide a comprehensive description of the multitude of morphological permutations. Indeed, even for a 'gothic' arch, to fully capture all its nuances and characteristics, a sophisticated approach that quantitatively combines all complex features in 3D is needed. Therefore, we applied a novel, validated 3D statistical shape analysis method (SSM) that quantitatively evaluates the ascending aorta/arch morphology as a single, contiguous 3D unit, without the need for manually measuring its numerous dimensions. (15 - 19) We hypothesized that unique 3D arch shape features extracted via the SSM are associated with left ventricular functional parameters and systemic blood pressure in patients late following isolated CoA repair.

Patients and Methods

Patient population and imaging

We analyzed routine follow-up CMR imaging data (1.5T Avanto MR scanner, Siemens Medical Solutions, Germany) of 53 asymptomatic patients late following isolated aortic coarctation repair (CoA; mean age 22.3±5.6 years, Table 1), including scans from 2007 to 2015 (Figure 1, left). The CMRs were obtained 12 to 38 years (mean 20.6±5.0 years) following initial CoA repair, and none had hemodynamically significant residual aortic arch obstruction or CoA requiring revision/reintervention as determined by Doppler echocardiographic interrogation. 36 patients had initial repair during the first year of life (68%), 7 patients in second year, and 10 patients more than 5 years after birth (with the oldest age at repair at 10 years). Patients with additional left-sided obstructive lesion (including hypoplastic left heart syndrome) or hypoplastic aortic arch/interrupted aortic arch were excluded, as well as those with aneurysmal dilatation and those with imaging artifacts due to stents or valve prosthesis. Approximately 80% of the cohort had an end-to-end (E-E) CoA repair, while nearly half had a bicuspid aortic valve (Table 1). Ethical approval was obtained for the use of image data for research, and all patients or legal guardians gave informed consent.

Left ventricular ejection fraction (LVEF), end diastolic volume (LVEDV) and ventricular mass (LVM) were calculated from the CMR short-axis stack (Table 1). Resting systolic blood pressure (BP) was measured during CMR acquisition using a cuff in the right arm. Body surface area (BSA) was calculated following the Haycock formula (20), and parameters were indexed with BSA, where appropriate, denoted with a preceding lower case *i* (i.e. iLVEDV and iLVM).

Aortic arch volumes were segmented and reconstructed from the CMR using a 3D balanced, steady-state free precession (bSSFP) whole-heart sequence during mid-diastole rest using

Active Contours segmentation tools (21). The 3D reconstructed surface models were exported as computational surface meshes, and were cut consistently with a plane below the aortic root (subannular) and at the level of the diaphragm using The Vascular Modeling Toolkit (VMTK, (22)). Head and neck vessels and coronary arteries were removed. Prior to 3D shape analysis, the obtained aortic arch shapes from all patients were pre-aligned on top of each other using an iterative closest point algorithm in VMTK. (23) The meshed, cut and aligned 3D arch surface models of all 53 aortic arches constituted the input for the statistical shape model (SSM) (Figure 1, left). (15)

Statistical shape analysis method (SSM)

The SSM approach was used to process and analyze all 3D shape information provided by the 53 aortic arch surface models in an integrated computational model, with no need for additional manual measurements or land-marking. (24, 25). Essentially, from the 53 meshes derived from the CMR, the SSM framework (Deformetrica, www.deformetrica.org) computes a *template* or *atlas*, i.e. the 3D anatomical mean shape as seen in Figure 1, right, blue. (18) From this template, each patient's aortic arch shape can be fully described by its unique, patient-specific set of deformation vectors ("forward approach") (26), that recreates each of the 53 patient arches by deforming the template aorta towards the patient shape. All sets of deformation vectors together numerically describe the 3D shape features present in the population, with no need for a collection of 2D measurements, coordinates, angles, points, or landmarks, thus allowing statistical analysis to assess how shape variability relates to clinical parameters. (15, 16)

Partial least squares regression (PLS) was applied to the computed deformation vectors, in order to extract 3D shape features (i.e. shape deformations) *most correlated* to the four clinical response parameters (LVEF, iLVEDV, iLVM and BP). (15, 19, 27) Prior to extracting shape features related to functional parameters, size effects due to differences in BSA between patients were removed via a first PLS regression, as described previously (15, 19). Each extracted shape feature can be visualized in 3D (28) by deforming the computed template shape along the extracted deformation vectors ("PLS modes") from low (-2 standard deviations, SD) to high (+2SD) values of the response parameter relative to the template. Furthermore, a *shape vector* is calculated which numerically quantifies how much of the extracted shape features related to the clinical parameter are contained within each patient's arch. (15, 27) Therefore, each patient's 3D shape information, initially provided as a multitude of deformation vectors, is broken down to one, unit-less number that represents the severity of the extracted shape feature within each of the 53 patients in relation to a functional clinical parameter. (15, 16, 19, 27)

The SSM template shape and patient-specific deformation vectors were thus computed. The template shape was validated as the representative mean shape of the 53-patient cohort in two ways. First, geometrically, by comparing gross geometric characteristics (volume V, surface area A_{surf} and centerline length L_{CL}) of the template against the respective mean values from the entire population extracted via VMTK. (15) Secondly, the template shape was validated numerically via 10-fold cross-validation: the dataset was divided randomly into 10 subsets and the template was re-computed 10 times based on a reduced dataset of 9 subsets, until each of the 10 subsets had been left out once, in order to verify independence of the included subjects. (27)

Traditional 3D morphometrics

In order to allow for an additional quantitative shape assessment of the derived shape patterns related to functional parameters, we measured traditional morphometric parameters on the computed 3D shapes and on the obtained template aorta (Mimics, Materialise, Leuven, Belgium): arch height h to width w ratio (h/w) just above the aortic root and, at the same level, the best fitting ascending and descending aortic diameter (D_{asc} and D_{desc} respectively) ratio (D_{asc}/D_{desc}).

Statistical Analysis

Associations between the four functional parameters (LVEF, iLVEDV, iLVM and BP) and the shape vectors describing 3D arch shape features were assessed via standard bi-variate correlation analyses. *Pearson's r* is reported for parametric, normally distributed data. Non-normality was assumed if the Shapiro-Wilk test was significant, assuming a significance level of $p<0.05$. For correlation analyses, computed p-values were adjusted for multiple comparisons via permutation tests with 100,000 permutations at α-level 0.05 (29). As PLS regression is sensitive to outliers (30), the Cook's distance (measuring the influence of a single subject on the final regression results) was computed for each PLS regression run. For all the PLS regression runs using functional parameters, two subjects exceeding four times the mean Cook's distance were considered to be influential and were subsequently removed from the respective shape feature extraction. Prior to extracting shape features related to functional parameters, size effects were removed by regressing the computed deformation vectors with BSA. One subject had to be removed from subsequent analyses for being influential to the regression, following the Cook's distance analysis.

Statistical tests were performed in Matlab and SPSS (IBM SPSS Statistics, SPSS Inc., USA).

Results

Template aortic arch

Qualitatively, the template aorta, derived as the mean 3D aorta shape computed from the 53-patient cohort, had a moderately increased height-to-width ratio and a non-angulated romanesque-type arch shape without any distinct narrowing or re-coarctation (Figure 1). These features were typical of what a surgeon or cardiologist would label as a 'perfect' aortic arch following CoA repair. As a validation, traditional morphometric parameters measured on the template shape were close to their respective mean values as calculated from the entire cohort (Table 2), with an overall deviation of 3.3% (individual deviations ΔV=5.6%, ΔA_{surf}=3.0%, and ΔL_{CL}=1.4%). In addition, cross-validation confirmed that removing subjects randomly from the population did not change the template shape significantly (average surface distance between original template shape and cross-validated shapes ΔD_{surf} = 0.285±0.07mm). The template was thus validated as a representative anatomic mean shape of our cohort.

Correlations between arch shape features with left ventricular function, volume, and mass

PLS regression results showed derived 3D shape vectors to be significantly correlated with LVEF, even after adjusting for multiple comparisons (r=0.42, p=0.024). Shape features that were associated with lower LVEF include an overall gothic-like aortic arch shape with elevated height-to-width ratio (h/w=1.33, Table 2) and an elongated ascending and shorter transverse arch and a slight size mismatch between a smaller isthmus and larger descending aorta. In contrast, a shorter, generally more rounded arch was associated with higher LVEF (h/w = 0.93; Figure 2). Moreover, the nearly identical aortic arch features associated with lower LVEF were also observed to correlate with both increased iLVEDV (h/w=1.73; r=0.65, p<0.001, Figure 3) and higher iLVM (h/w=1.47; r=0.44, p=0.014, Figure 4). Conversely, aortic arches associated with both low iLVEDV and low iLVM featured an overall more compact and rounded (romanesque) arch shape (h/w=0.73 and 0.70, respectively) with a larger ascending arch that tapers into a relatively smaller distal transverse and isthmus arch continuation (D_{asc}/D_{desc}=1.73 and 1.96, respectively).

Correlations of arch shape features with systolic blood pressure at rest

High systolic resting BP was identified with a gothic-type arch shape (h/w=1.41) presenting with a mild ascending arch dilation and a narrow and short transverse arch with exaggerated acute angulation at its apex, followed by mild diameter increase from isthmus to descending aorta (Figure 5). The aortic arch shape associated with low BP showed a more crenel-like, longer and rounded aortic arch. While initially significant in stand-alone statistic, this shape to BP association did not reach statistical significance after adjusting for multiple comparisons (r=0.32, p=0.160).

Discussion

The goal of surgical repair of CoA is to restore unobstructed systemic blood flow through the aortic arch, with the additional beneficial consequence of life-long freedom from hypertension. However, an observation is emerging that a significant number of patients late after what appeared to be successful CoA repair with no residual obstructive lesion suffer from systemic hypertension and exaggerated blood pressure response to exercise. (3-6) While intrinsic abnormal aortic wall properties exist in patients with aortic arch anomalies, investigations into the role of arterial elastance and compliance have not yielded definitive mechanistic link with systemic hypertension in patients following CoA repair. Recently, the appearance of the aortic arch in patients following CoA repair has been called into question as a potential contributor to poor late outcomes. (2) Again, traditional linear 2D measurements have led to conflicting results. There is no question that the aortic arches in patients who had CoA repair look different from those of healthy individuals. This is confounded by the fact that not only different operative techniques exist, but the entire ascending aorta-aortic arch-isthmus-descending aorta complex can vary greatly in size and shape from patient to patient, in addition to differing incidences of residual arch obstruction, dilatation, and tortuosity. Therefore, to accurately capture all the features within an aortic arch following CoA repair requires a sophisticated analysis of its modified (i.e. repaired) and unmodified (i.e. native) characteristics in 3D space.

In this study, using a novel 3D statistical shape analysis method (SSM) that is capable of extracting and visualizing complex aortic arch shape features, unique aortic arch features late following CoA repair were found to correlate with poorer left ventricular function and increased left ventricular volume and mass. This methodology, which combines CMR-based computational modeling and advanced statistical analysis, is based on defining a mean aortic arch that is representative of the average shape from a specific patient cohort. Adopting a template aorta based on subjects with normal hearts and normal aortic arches would be meaningless for CoA patients due to the compulsory aortic arch reconstruction and the known variations in arch geometry among these patients. Therefore, the template aorta (Figure 1) is derived from the 53-patient cohort as the 'norm' for a CoA patient, with a smooth 'candy-cane'-like curvature that extends from the ascending aorta to the descending. Free from obvious obstruction or acute changes in size and cross sectional area, this template would typically be one that surgeons and cardiologists would consider a successful repaired aortic arch.

From this template, the SSM quantified shape features or deformation vectors that correlated with lower LVEF, larger iLVEDV and higher iLVM. This suggests that independent of hemodynamically important residual obstruction, stenosis or hypoplasia, how the aortic arch is shaped can be associated with poorer left ventricular performance. It appears that the common features linked with these worse left ventricular functional parameters are aortic arches with elongated ascending aorta, increased height-to-width ratio, and shorter transverse arch and a slight size mismatch between a smaller isthmus and larger descending aorta. Interestingly, common features observed in those aortic arches associated with better left ventricular parameters included overall smaller arch complex, slightly oversized ascending aorta, more rounded and longer transverse arch, and smoother match between isthmus to descending aorta. However, it should be noted that all the patients were asymptomatic from heart failure. Indeed, the lowest LVEF in the cohort was 52%, and highest iLVM and iLVEDV were within acceptable limits. Nonetheless, the combination of higher left ventricular mass and volume are known to be risk markers for increased cardiovascular morbidity, including coronary artery disease and cerebral vascular accidents. (4, 31)

While residual arch stenosis has been previously associated with higher iLVM by Ong et al (7), the strong correlation uncovered in this study highlighted the importance of shape alone, independent of flow obstruction, could play a role in late CoA outcomes. Along the same vein, our study also examined, for the first time, the role of the overall proportion of the intrathoracic aorta. With the aortic arch geometry reconstruction uniformly obtained from the aortic root to the diaphragm in each patient, and influence of different body size eliminated, smaller and more compact, rounded arches seemed to be associated with better left ventricular function. Yet, overall arch size cannot be accounted for when using traditional morphometric. Therefore, the overall intrathoracic aorta size appears to be relevant, further justifying assessing the 3D shape anatomy contiguously in whole.

The trend that elevated resting blood pressure was associated with a gothic-type aortic arch shape was in line with other studies, some of which also showed association with exaggerated blood pressure response to exercise. (32, 33) Presence of abnormal wall properties of the entire systemic arterial tree, such as reduced compliance and distensibility, has been shown previously to exist in CoA patients with hypertension. (5, 6, 34) The present shape analysis methodology cannot account for aortic wall property variations, which could potentially confound the association between arch shape and hypertension. Combined with our recent development of wave intensity analysis which can evaluate arterial wall distensibility and elastance, it is possible in the future that these two CMR-derived methods can reveal a clearer relationship between aortic arch shape and hypertension.

Lastly, it is worth to highlight the similarity and difference seen between aortic arch shape features in CoA patients and those in patients following the Norwood procedure for hypoplastic left heart syndrome (HLHS). In a recent study applying the same methodology in HLHS patients following the Norwood-type aortic arch reconstruction (16), we described a significant correlation between unique aortic arch shape features and increased right ventricular end-diastolic volume and other adverse outcomes. While these two studies concurrently demonstrate the possible importance of aortic arch shape, there is a major difference: the aortic arch shape and morphology following the Norwood procedure are potentially modifiable, but those in CoA patients after successful repair are more difficult to modify. The technique/manner in which the combination of Damus-Kay-Stansel/arch reconstruction is performed at Stage One Norwood is clearly a major determinant on the eventual shape of the aortic arch in HLHS patients. However, as seen in this study, the deterministic factors in the shape features of an aortic arch late following CoA repair are essentially intrinsic or inherently altered, i.e. a gothic or romanesque aortic arch is born that way. In the absence of obvious hypoplasia or stenosis, one typically would not surgically intervene on a gothic-appearing aortic arch, nor would one reconstruct an arch that we have identified to be associated with the worse left ventricular parameters. In fact, in reviewing the CT or MR of a patient, prior to this study, one would have likely described such an aortic arch to be a 'successful' CoA repair.

Despite uncovering these previously unknown relationships between aortic shape and clinical parameters in patients following CoA repair, it is important to note that this study does not reveal any mechanistic insight as to why specific distortion or deformation in some shape features would be important, and thus cannot provide a causal relationship to our observations. Whether these deranged aortic shapes lead to altered impedance and/or perturbed aortic outflow is unknown. Further studies, perhaps with 4-D CMR (35) and advanced computational fluid dynamics modeling, where realistic time-dependent and pulsatile flow/pressure characteristics can be simulated and examined, may yield important insights into the flow disturbances that can lead to worse cardiac function and clinical outcomes.

Conclusions

In this study, we assessed aortic arch morphology post CoA repair using a novel statistical shape modeling approach in order to extract three-dimensional arch shape features related to functional parameters acquired during routine follow-up magnetic resonance assessment. We found a previously unknown association of unique aortic arch shape with lower left ventricular ejection fraction and elevated left ventricular end diastolic volume and mass. Moreover, our study suggested a gothic aortic arch might be correlated with hypertension, but this was not conclusive. Nonetheless, this study did confirm aortic arch shape in patients post CoA repair could be related to cardiac function, and in so doing it also highlighted that a few isolated 2D morphometric measurement could not fully capture the intricate and complex combination of shape features in an aortic arch. Adaptation of the statistical shape analysis method using extracted three-dimensional aortic arch geometry might provide a predictive tool to risk stratify patients following successful CoA repair for late development of hypertension and left ventricular functional derangements.

Acknowledgements and Disclosures

This report incorporates independent research from the National Institute for Health Research Biomedical Research Centre Funding Scheme. The views expressed in this publication are those of the author(s) and not necessarily those of the NHS, the National Institute for Health Research or the Department of Health.

The authors gratefully acknowledge support from Fondation Leducq, FP7 integrated project MD-Paedigree (partially funded by the European Commission) and National Institute of Health Research UK (NIHR).

The authors have nothing to disclose with regard to commercial support.

References (*max. 35*)

1. Hauser M. Exercise blood pressure in congenital heart disease and in patients after coarctation repair. Heart. 2003 Feb 1;89(2):125–6.

2. De Caro E, Trocchio G, Smeraldi A, Calevo MG, Pongiglione G. Aortic Arch Geometry and Exercise-Induced Hypertension in Aortic Coarctation. The American Journal of Cardiology. 2007 Mai;99(9):1284–7.

3. Puranik R, Tsang VT, Puranik S, Jones R, Cullen S, Bonhoeffer P, et al. Late magnetic resonance surveillance of repaired coarctation of the aorta. Eur J Cardiothorac Surg. 2009 Jul 1;36(1):91–5.

4. Brown ML, Burkhart HM, Connolly HM, Dearani JA, Cetta F, Li Z, et al. Coarctation of the Aorta: Lifelong Surveillance Is Mandatory Following Surgical Repair. Journal of the American College of Cardiology. 2013 Sep 10;62(11):1020–5.

5. O'Sullivan J. Late Hypertension in Patients with Repaired Aortic Coarctation. Curr Hypertens Rep. 2014 Mar 1;16(3):1–6.

6. Canniffe C, Ou P, Walsh K, Bonnet D, Celermajer D. Hypertension after repair of aortic coarctation — A systematic review. International Journal of Cardiology. 2013 Sep 10;167(6):2456–61.

7. Ong CM, Canter CE, Gutierrez FR, Sekarski DR, Goldring DR. Increased stiffness and persistent narrowing of the aorta after successful repair of coarctation of the aorta: Relationship to left ventricular mass and blood pressure at rest and with exercise. American Heart Journal. 1992 Jun;123(6):1594–600.

8. Vriend JWJ, Zwinderman AH, Groot E de, Kastelein JJP, Bouma BJ, Mulder BJM. Predictive value of mild, residual descending aortic narrowing for blood pressure and vascular damage in patients after repair of aortic coarctation. European Heart Journal. 2005 Jan 1;26(1):84–90.

9. Weber HS, Cyran SE, Grzeszczak M, Myers JL, Gleason MM, Baylen BG. Discrepancies in aortic growth explain aortic arch gradients during exercise. Journal of the American College of Cardiology. 1993 März;21(4):1002–7.

10. Lee MGY, Kowalski R, Galati JC, Cheung MMH, Jones B, Koleff J, et al. Twenty-four-hour ambulatory blood pressure monitoring detects a high prevalence of hypertension late after coarctation repair in patients with hypoplastic arches. The Journal of Thoracic and Cardiovascular Surgery. 2012 Nov;144(5):1110–8.

11. Ou P, Bonnet D, Auriacombe L, Pedroni E, Balleux F, Sidi D, et al. Late systemic hypertension and aortic arch geometry after successful repair of coarctation of the aorta. European Heart Journal. 2004 Oct 1;25(20):1853–9.

12. Ou P, Celermajer DS, Mousseaux E, Giron A, Aggoun Y, Szezepanski I, et al. Vascular Remodeling After "Successful" Repair of Coarctation: Impact of Aortic Arch Geometry. Journal of the American College of Cardiology. 2007 Feb 27;49(8):883–90.

13. Ou P, Celermajer DS, Raisky O, Jolivet O, Buyens F, Herment A, et al. Angular (Gothic) aortic arch leads to enhanced systolic wave reflection, central aortic stiffness, and increased left ventricular mass late after aortic coarctation repair: Evaluation with magnetic resonance flow mapping. The Journal of Thoracic and Cardiovascular Surgery. 2008 Jan;135(1):62–8.

14. Ntsinjana HN, Biglino G, Capelli C, Tann O, Giardini A, Derrick G, et al. Aortic arch shape is not associated with hypertensive response to exercise in patients with repaired congenital heart diseases. Journal of Cardiovascular Magnetic Resonance. 2013 Nov 12;15(1):101.

15. Bruse JL, McLeod K, Biglino G, Ntsinjana HN, Capelli C, Hsia T-Y, et al. A statistical shape modelling framework to extract 3D shape biomarkers from medical imaging data: assessing arch morphology of repaired coarctation of the aorta. BMC Med Imaging. 2016;16:40.

16. Bruse JL, Cervi E, McLeod K, Biglino G, Sermesant M, Pennec X, et al. Looks do matter! Aortic arch shape following hypoplastic left heart syndrome palliation correlates with cavopulmonary outcomes. Ann Thorac Surg. 2016 Jun (*in Press*)

17. Leonardi B, Taylor AM, Mansi T, Voigt I, Sermesant M, Pennec X, et al. Computational modelling of the right ventricle in repaired tetralogy of Fallot: can it provide insight into patient treatment? Eur Heart J Cardiovasc Imaging. 2013 Apr;14(4):381–6.

18. Durrleman S, Prastawa M, Charon N, Korenberg JR, Joshi S, Gerig G, et al. Morphometry of anatomical shape complexes with dense deformations and sparse parameters. NeuroImage. 2014 Nov 1;101:35–49.

19. Bruse JL, McLeod K, Biglino G, Ntsinjana HN, Capelli C, Hsia T-Y, et al. A Non-parametric Statistical Shape Model for Assessment of the Surgically Repaired Aortic Arch in Coarctation of the Aorta: How Normal is Abnormal? In: O Camara et al (Eds): Statistical Atlases and Computational Models of the Heart 2015. Munich: Springer International Publishing Switzerland 2016; 2016. p. 21–9. (Image Processing, Computer Vision, Pattern Recognition, and Graphics; vol. LNCS 9534).

20. Haycock GB, Schwartz GJ, Wisotsky DH. Geometric method for measuring body surface area: A height-weight formula validated in infants, children, and adults. The Journal of Pediatrics. 1978 Jul;93(1):62–6.

21. Yushkevich PA, Piven J, Hazlett HC, Smith RG, Ho S, Gee JC, et al. User-guided 3D active contour segmentation of anatomical structures: Significantly improved efficiency and reliability. NeuroImage. 2006 Jul 1;31(3):1116–28.

22. Antiga L, Piccinelli M, Botti L, Ene-Iordache B, Remuzzi A, Steinman DA. An image-based modeling framework for patient-specific computational hemodynamics. Med Biol Eng Comput. 2008 Nov 1;46(11):1097–112.

23. Besl PJ, McKay ND. A method for registration of 3-D shapes. IEEE Transactions on Pattern Analysis and Machine Intelligence. 1992 Feb;14(2):239–56.

24. Young AA, Frangi AF. Computational cardiac atlases: from patient to population and back. Exp Physiol. 2009 May 1;94(5):578–96.

25. Durrleman S, Pennec X, Trouvé A, Ayache N. Statistical models of sets of curves and surfaces based on currents. Medical Image Analysis. 2009 Oct;13(5):793–808.

26. Durrleman S, Pennec X, Trouvé A, Ayache N. A forward model to build unbiased atlases from curves and surfaces. In 2008.

27. Mansi T, Voigt I, Leonardi B, Pennec X, Durrleman S, Sermesant M, et al. A Statistical Model for Quantification and Prediction of Cardiac Remodelling: Application to Tetralogy of Fallot. IEEE Transactions on Medical Imaging. 2011;30(9):1605–16.

28. Ahrens J, Geveci B, Law C. ParaView: An End-User Tool for Large-Data Visualization. The Visualization Handbook. 2005;717.

29. Groppe DM, Urbach TP, Kutas M. Mass univariate analysis of event-related brain potentials/fields I: A critical tutorial review. Psychophysiology. 2011 Dec;48(12):1711–25.

30. Daszykowski M, Kaczmarek K, Vander Heyden Y, Walczak B. Robust statistics in data analysis — A review: Basic concepts. Chemometrics and Intelligent Laboratory Systems. 2007 Feb 15;85(2):203–19.

31. Levy D, Garrison RJ, Savage DD, Kannel WB, Castelli WP. Prognostic Implications of Echocardiographically Determined Left Ventricular Mass in the Framingham Heart Study. New England Journal of Medicine. 1990 Mai;322(22):1561–6.

32. Donazzan L, Crepaz R, Stuefer J, Stellin G. Abnormalities of Aortic Arch Shape, Central Aortic Flow Dynamics, and Distensibility Predispose to Hypertension After Successful Repair of Aortic Coarctation. World Journal for Pediatric and Congenital Heart Surgery. 2014 Oct 1;5(4):546–53.

33. Ou P, Mousseaux E, Celermajer DS, Pedroni E, Vouhe P, Sidi D, et al. Aortic arch shape deformation after coarctation surgery: Effect on blood pressure response. The Journal of Thoracic and Cardiovascular Surgery. 2006 Nov;132(5):1105–11.

34. Lombardi KC, Northrup V, McNamara RL, Sugeng L, Weismann CG. Aortic Stiffness and Left Ventricular Diastolic Function in Children Following Early Repair of Aortic Coarctation. The American Journal of Cardiology. 2013 Dezember;112(11):1828–33.

35. Frydrychowicz A, Markl M, Hirtler D, Harloff A, Schlensak C, Geiger J, et al. Aortic Hemodynamics in Patients With and Without Repair of Aortic Coarctation: In Vivo Analysis by 4D Flow-Sensitive Magnetic Resonance Imaging. Investigative Radiology May 2011. 2011;46(5):317–25.

Table 1

Overview of patient characteristics (BSA = body surface area; TAV = tricuspid aortic valve; BAV = bicuspid aortic valve; fBAV = functionally bicuspid aortic valve; E-E = end-to-end anastomosis; ExtE-E = extended end-to-end anastomosis; LVEF = left ventricular ejection fraction; iLVEDV = indexed left ventricular end-diastolic volume; iLVM = indexed left ventricular mass; BP = systolic resting blood pressure). Lower case *i* indicates parameters indexed to patient BSA.

Variables	*Mean±Standard Deviation (range)*
Number of Patients	53
Age at time of CMR [Years]	22.3±5.6 (15.1-38.1)
Height [cm]	170.5±9.5 (147-188)
BSA [m²]	1.83±0.21 (1.44-2.22)
Aortic Valve Morphology (TAV/BAV/fBAV)	(21/26/6)
Type of Initial Repair (E-E/ExtE-E/Flap/Patch/Balloon)	(42/1/6/3/1)
LVEF [%]	64.1±7.3 (52-78)
iLVEDV [ml/m²]	78.5±14.6 (57-108)
iLVM [g/m²]	64.1±14.7 (37-94)
BP [mmHg]	130.0±17.1 (92-163)

Table 2

Morphometric parameters measured on the computed 3D shapes and respective population averages. (A_{surf} = arch surface area; V = volume; L_{CL} = centerline length; L_{To} = centerline tortuosity; D_{av} = average diameter along the centerline; D_{asc}/D_{desc} = ascending to descending diameter ratio; h/w = arch height to width ratio).

3D Shape	*V [mm³]*	*Asurf [mm²]*	*L_{CL} [mm]*	*L_{To}*	*D_{av} [mm]*	*D_{asc}/D_{desc}*	*h/w*
Low LVEF Shape	97804	18408	253.65	1.85	20.90	1.11	1.33
High LVEF Shape	75583	14598	207.85	1.64	19.62	1.50	0.93
Low iLVEDV Shape	72193	13607	190.48	1.52	19.71	1.73	0.73
High iLVEDV Shape	106257	19824	268.62	1.95	20.78	1.08	1.43
Low iLVM Shape	69599	13042	183.12	1.66	19.25	1.96	0.70
High iLVM Shape	117210	21145	276.04	1.81	21.32	0.96	1.47
Low BP Shape	87759	16873	234.81	1.64	20.48	1.15	0.97
High BP Shape	85570	16177	228.24	1.87	20.05	1.41	1.29
Template	88108	16665	230.84	1.74	20.56	1.32	0.94
Population Average	*93111*	17166	*233.96*	*1.80*	*19.40*	-	-

Figure Legends

Figure 1: Reconstructed 3D surface models of 53 aortic arches post coarctation repair included in this study (grey, left) and computed mean anatomic reference shape based on the input shape population (template shape, blue, right).

Figure 2: Visualization of 3D aortic arch shape patterns associated with LVEF, deforming the template shape from low (-2SD) to high (+2SD) values of the response parameter LVEF (computed shape features visualized in blue), and definition of height to width ratio h/w (a). Color maps show local 3D shape deviations as distance in millimeters between the computed shapes and the template shape, overlaid in grey; blue colors relate to inwards deformations; red colors to outwards deformations from the template (b). Standard bi-variate correlation analysis was used to evaluate numerically how strongly the found patterns were related to LVEF (c). Low (normal) LVEF thereby was associated with an overall large arch with high h/w ratio, a slim ascending and mildly hypoplastic transverse arch, while high LVEF related to more rounded and compact arches.

Figure 3: Elevated iLVEDV was associated with overall larger and tortuous arches with high h/w ratio, a long, slim ascending and proximally hypoplastic transverse aortic arch. Extracted shape patterns are visualized as deformations of the template in blue (a), local deviations from the template shape are shown as color maps in (b).

Figure 4: Elevated iLVM was associated with an overall large and tortuous, high h/w ratio arch shape, showing a very slim ascending and transverse arch with mild narrowing at the isthmus region and a long and dilated descending aorta. Extracted shape patterns are visualized as deformations of the template in blue (a), local deviations from the template shape are shown as color maps in (b).

Figure 5: High systolic resting BP related to an overall gothic-type and tortuous arch shape with mildly dilated ascending aorta and signs of residual narrowing at the isthmus section,

compared to a crenel-like arch for lower BP values. Yet, results were not significant after adjusting for multiple comparisons. Extracted shape patterns are visualized as deformations of the template in blue (a), local deviations from the template shape are shown as color maps in (b).

Video 1: Video showing the deformation of the computed template aorta (overlaid in grey) along the derived PLS shape mode for iLVEDV from -2SD to +2SD; thus visualizing the 3D aortic arch shape features most associated with low and high iLVEDV, respectively.

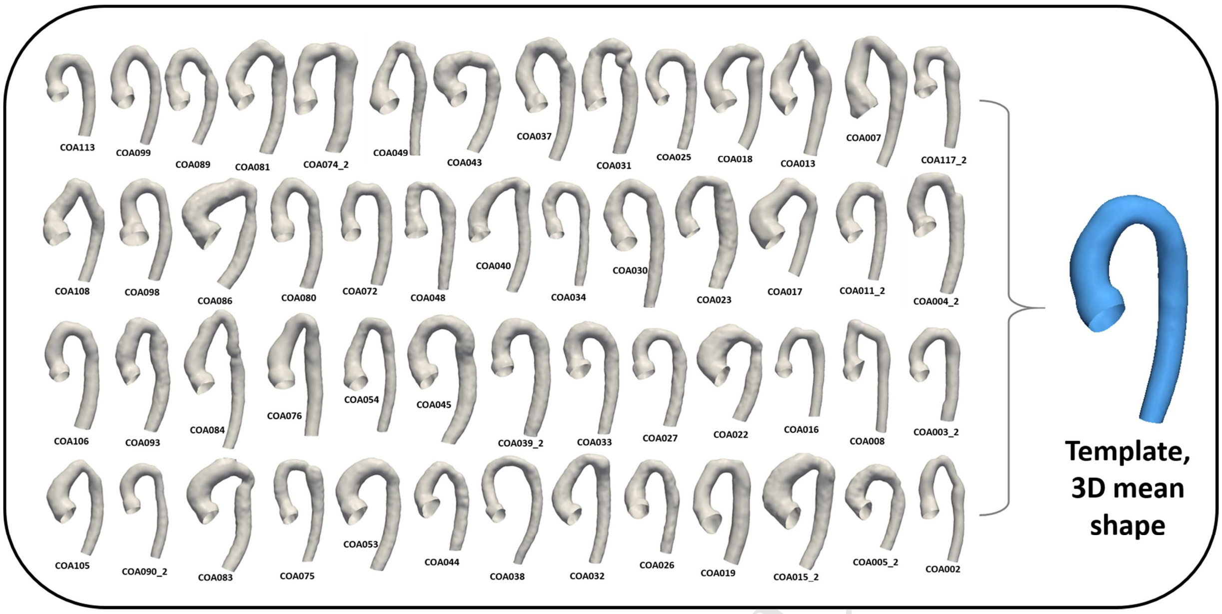
COA113
COA099
COA089
COA081
COA074_2
COA049
COA043
COA037
COA031
COA025
COA018
COA013
COA007
COA117_2
COA108
COA098
COA086
COA080
COA072
COA048
COA040
COA034
COA030
COA023
COA017
COA011_2
COA004_2
COA106
COA093
COA084
COA076
COA054
COA045
COA039_2
COA033
COA027
COA022
COA016
COA008
COA003_2
COA105
COA090_2
COA083
COA075
COA053
COA044
COA038
COA032
COA026
COA019
COA015_2
COA005_2
COA002
Template, 3D mean shape

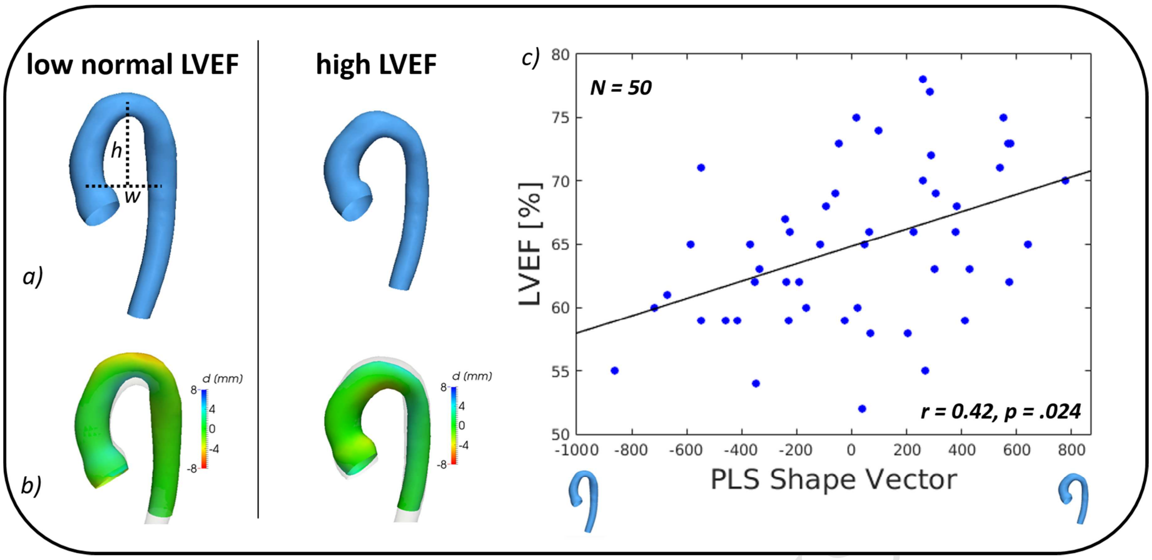

low normal LVEF
high LVEF
h
w
a)
b)
d (mm)
8
4
0
-4
-8
c)
N = 50
r = 0.42, p = .024
LVEF [%]
PLS Shape Vector
80
75
70
65
60
55
50
-1000
-800
-600
-400
-200
0
200
400
600
800

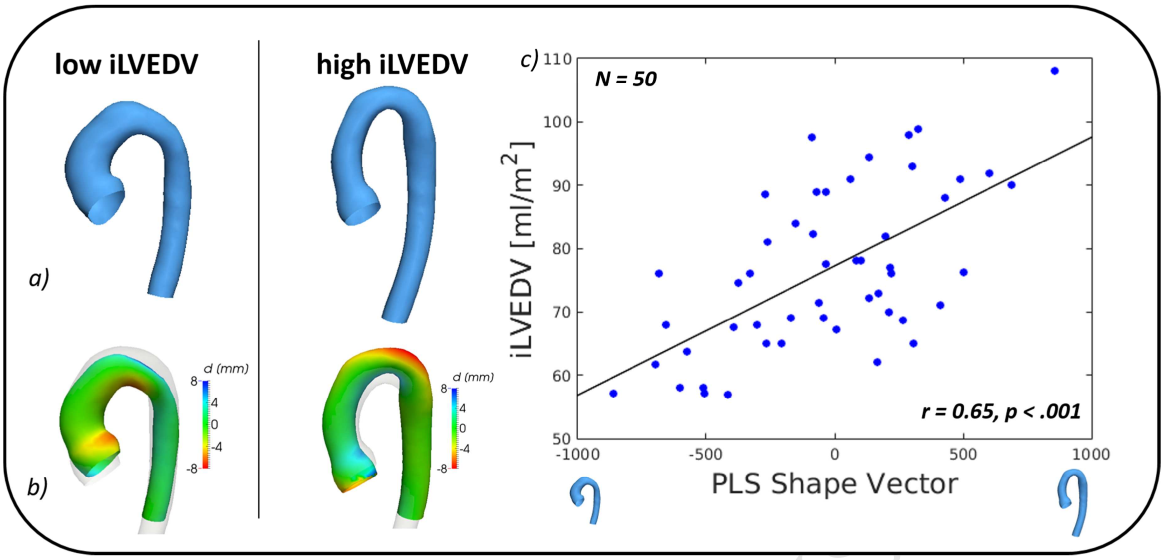
low iLVEDV
high iLVEDV
a)
b)
d (mm)
8
4
0
-4
-8
c)
N = 50
iLVEDV [ml/m2]
PLS Shape Vector
r = 0.65, p < .001
110
100
90
80
70
60
50
-1000
-500
0
500
1000

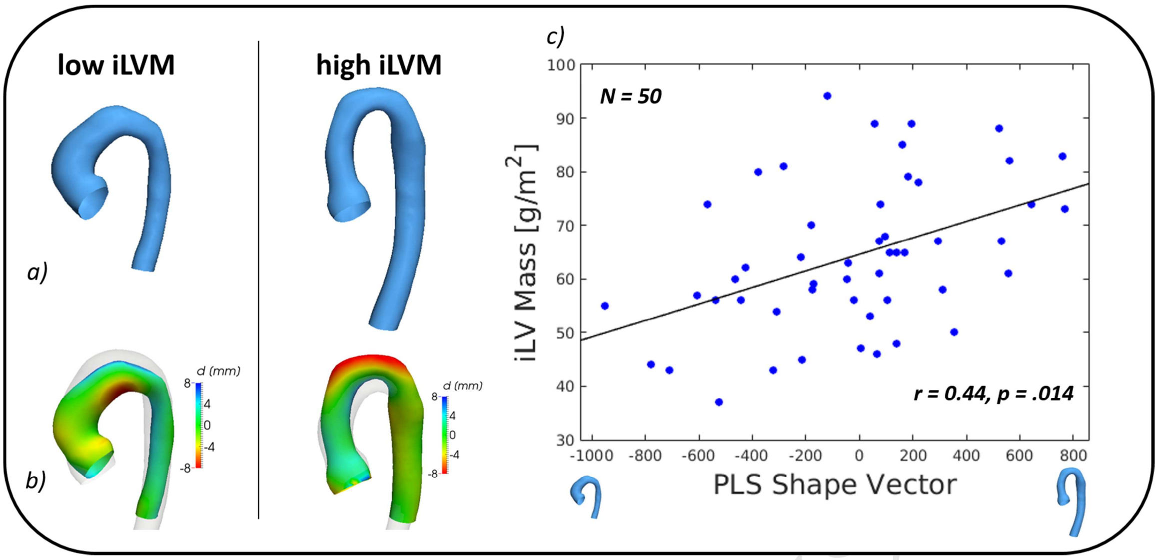

low iLVM
high iLVM
a)
b)
d (mm)
8
4
0
-4
-8
c)
N = 50
iLV Mass [g/m2]
r = 0.44, p = .014
PLS Shape Vector

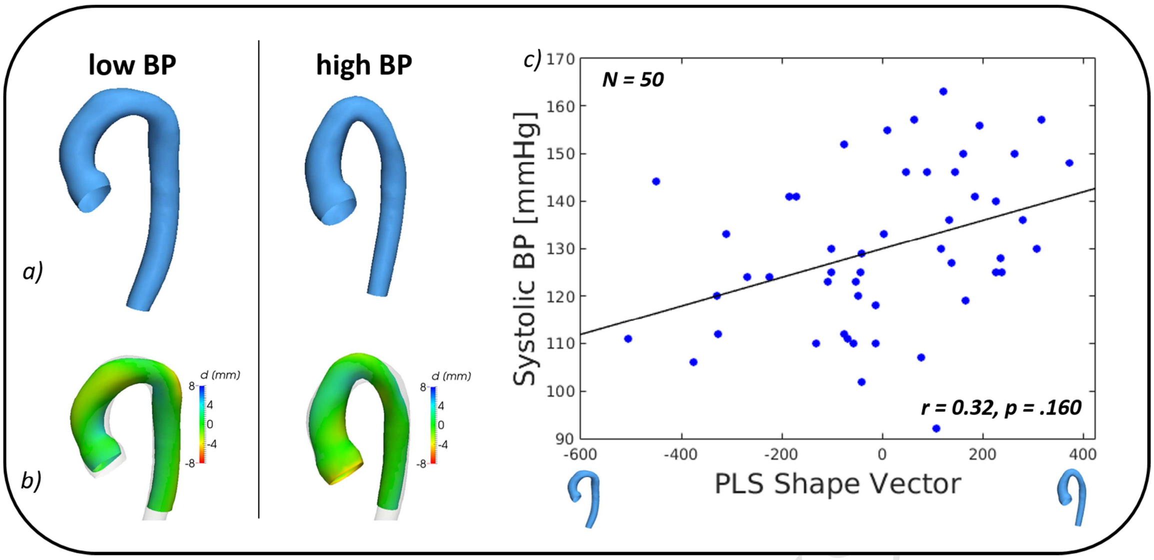
low BP
high BP
a)
b)
d (mm)
8
4
0
-4
-8
c)
N = 50
r = 0.32, p = .160
Systolic BP [mmHg]
PLS Shape Vector
170
160
150
140
130
120
110
100
90
-600
-400
-200
0
200
400

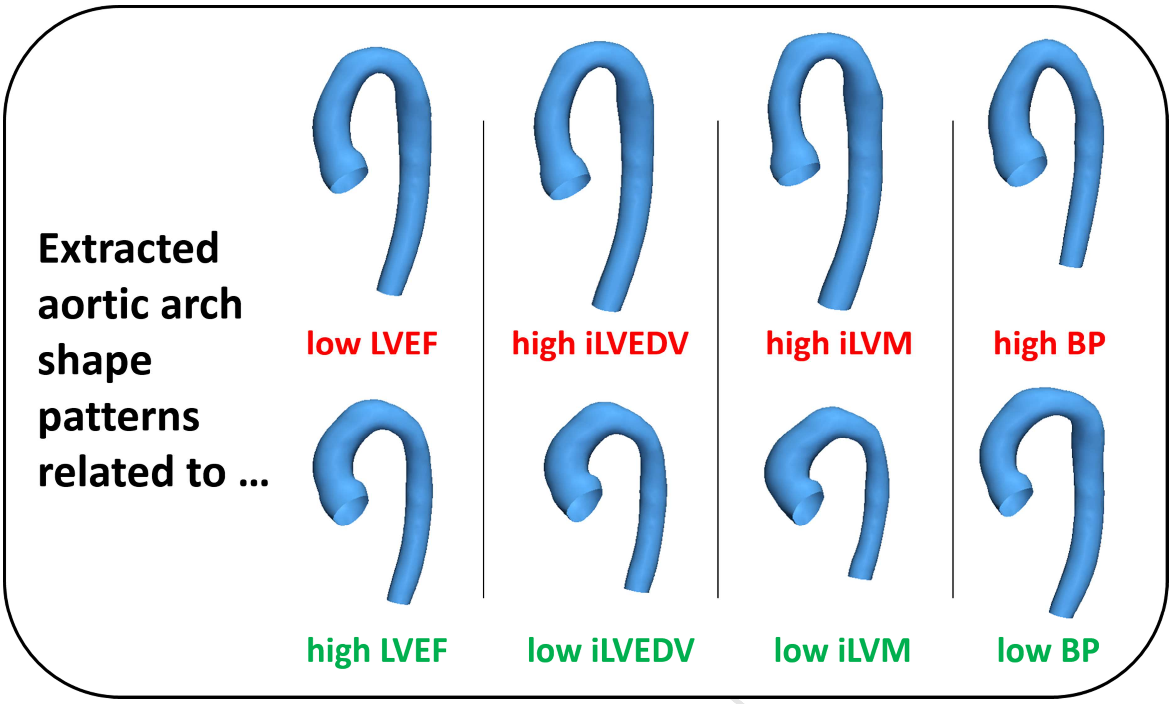
Extracted aortic arch shape patterns related to ...
low LVEF
high iLVEDV
high iLVM
high BP
high LVEF
low iLVEDV
low iLVM
low BP